Amplification of spin-transfer torque in magnetic tunnel junctions with an antiferromagnetic barrier

Yihong Cheng, Weigang Wang, and Shufeng Zhang[*]

Department of Physics, University of Arizona, Tucson, Arizona 85721, USA

We theoretically study spin-transfer torques in magnetic tunnel junctions (MTJs) with an antiferromagnetic insulator (AFI) as the tunnel barrier. When a finite voltage bias is applied to the MTJ, the energy relaxation of the tunnel electrons leads to asymmetric heating of two metallic layers. Consequently, there would be a magnon current flowing across the AFI layer, resulting a magnon transfer torque in addition to the electron spin-transfer torque. Comparing to MTJs with a nonmagnetic insulator which prohibits the magnon transmission, we find the magnon transfer torque with an AFI barrier could be several times larger than the conventional spin-transfer torque of the tunnel electrons. This study presents a potential method to realize more efficient switching in MTJs and provides a motivation of experimental search for AFI-based MTJs.

I. INTRODUCTION

In today's spin-based information storage technology, magnetic tunnel junctions (MTJs) [1–4] have been arguably the most important building blocks. Since the discovery of large tunnel magnetoresistance (TMR) in the MgO-based MTJs about 14 years ago [5–8], research and development on MTJs have almost exclusively focused on MgO barriers. Indeed, MgO tunnel barriers have shown tremendous advantages over other insulating barriers such as amorphous Al_2O_3. The superior epitaxial growth of MgO barrier with transition metal ferromagnet (FM) electrodes makes the tunnel resistance rather tunable to meet the different requirement of specific devices, e.g., magnetic reading heads and magnetic random access memories (MRAMs) [9]. Most importantly, TMR of MgO-based MTJs is as large as 600% at room temperature [10], far exceeding other known tunnel barriers.

While the large TMR value of MgO-based MTJs provides unprecedented efficiency for magnetic reading, switching the magnetization direction of MTJs for the writing remains challenging. In the first generation of MRAM devices, an external magnetic field is used for magnetization switching; this method is not scalable and would fail for high density MRAMs [11]. The second generation takes advantage of spin-transfer torques (STTs) where a sufficient large electric current across the tunnel barrier can reorient the relative magnetizations of two magnetic layers in parallel or antiparallel, depending on the polarity of the current [12–18]. Up until now, the critical switching current density (j_c) is very high, of the order of 10^6 A cm^{-2}. In the STT switching, the spin angular momentum of tunnel electrons from one electrode to the other determines the total magnetic torque. Under a typical switching voltage across the junction about 0.5 V, each tunneling electron transfers its spin angular momentum at a maximum of $\hbar/2$, but the accompanied energy of 0.5 eV

is completely wasted. Thus, the STT switching by tunnel electrons are not energy efficient.

In this paper we theoretically investigate the tunnel transport with an antiferromagnetic insulator (AFI) as tunnel barrier. Our central idea and motivation for replacing MgO by an AFI barrier are outlined below. Consider a tunnel junction made of two ferromagnetic metals separated by a thin antiferromagnetic insulator, as shown in Fig. 1. When a voltage is applied across the tunnel barrier, electrons tunnel from the electrode with the lower voltage to that with the higher voltage. While the tunneling electron will relax its energy in both electrodes, the majority of the energy is relaxed in the electrode receiving the tunnel electron. Since the inelastic mean free path is only a few angstroms for the tunnel electron with the energy about 0.5 eV above the Fermi level [19,20], the heat is generated near the vicinity of the interface. The heat is subsequently diffusing into the interior of the electrode as well as across the barrier. In the steady state condition, a temperature gradient is established in the structure and one expects a temperature difference would be created at the two sides of the barrier. It has been experimentally and theoretically shown that the temperature difference could reach a fraction of a Kelvin degree for a bias voltage of 0.5–1 V [21,22]. Consequently, a magnon current would flow across the AFI barrier from one FM electrode to the other, exerting a magnon transfer torque on the free magnetization layer. Theoretically, the magnon current driven by temperature gradient has already been studied in detail [23–27].

The above discussion leads us to critically examine whether it is possible to recycle the wasted energy of tunnel electrons for magnetization switching. Since a magnetic barrier is required for magnon propagation, both ferromagnetic and antiferromagnetic insulators would be barrier candidates. However, the ferromagnetic insulator would be strongly coupled with ferromagnetic electrodes and thus it is difficult to freely rotate the relative orientation of the magnetization of two electrodes. An antiferromagnetic barrier would be ideal: one can control and minimize the exchange bias and the
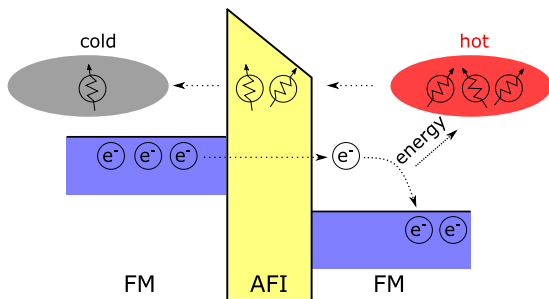
---
[*]zhangshu@email.arizona.edu

FIG. 1. Schematics of the proposed AFI-MTJ. Two FM layers are separated by an AFI barrier and they are biased by a negative voltage of the order of several hundreds of millivolts. Hot electrons tunnel from the left FM electrode to the right FM electrode and the excess energy is dissipated over inelastic scattering length to heat up magnons on the right. The resulting magnons would diffuse from right (hot) to left (cold) mediated by the magnons in AFI.

antiferromagnetic material is a theoretically and experimentally proven material which can efficiently propagate the magnon current [28–36].

The paper is organized as follows. In Sec. II we calculate the position-dependent temperature of the tunnel junction as a function of the bias voltage and current density. The magnon transfer torques due to temperature gradient is calculated in Sec. III, followed by numerical estimation on the amplification of the spin torque with the AFI barrier in Sec. IV. We conclude the paper in Sec. V.

II. HEAT TRANSPORT AND TEMPERATURE PROFILE

To model the temperature profile, we specify the geometrical parameters in Fig. 2(a): the MTJ, made of a pinned magnetic layer FM1, an AFI barrier, and a free magnetic layer FM2, is sandwiched by two nonmagnetic (NM) layers (representing the overlayer and underlayer of MTJs) so that the temperature profile is not simply limited within the MTJ. Thicknesses of the layers are labeled in Fig. 2(b). A time-dependent electric current $j_e(t)$ flows perpendicularly to the layers with a bias voltage $V(t)$ across the junction. The sign convention for the current is $j_e(t) < 0$ [or equivalently $V(t) < 0$] corresponding to net electron tunneling from FM1 to FM2.

We model the heat transport by using the layer-by-layer approach. In each layer, the heat diffusion equation reads

$$\rho_i C_i \frac{\partial T(t,x)}{\partial t} - \kappa_i \frac{\partial^2 T(t,x)}{\partial x^2} = P_i(t,x), \tag{1}$$

where ρ_i, C_i, and κ_i are the mass density, heat capacity, and thermal conductivity of the ith layer, and $P_i(t,x)$ is the power of heat source generated by the electric current. The Joule heating j_e^2/σ_i is always present for each metallic layer where σ_i is electric conductivity. In the tunnel junction, as illustrated in Fig. 1, the main energy relaxation of the tunnel electrons occurs near the interface. For the electrode receiving the tunnel electrons, the energy of tunnel electrons is above the Fermi level up to the bias voltage $V(t)$. These hot electrons have short mean free paths, of the order of 1 nm. For the electrode emitting electrons, the holes left by the tunnel electrons are
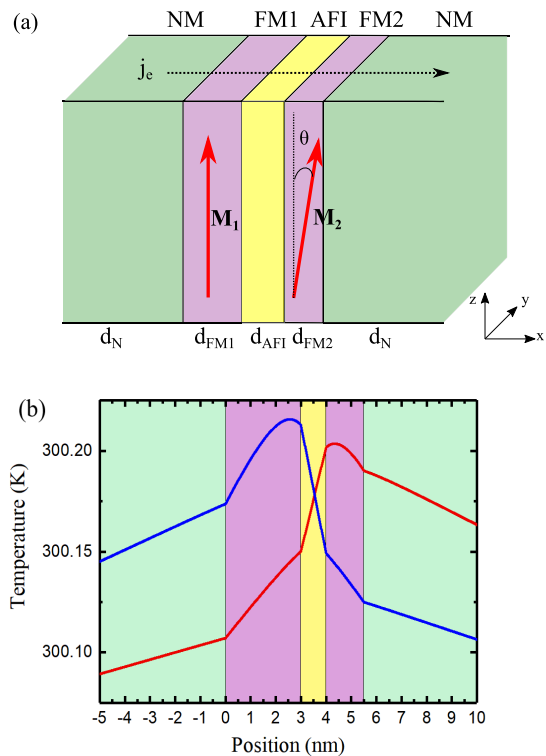

FIG. 2. (a) Proposed AFI-MTJ structure and (b) temperature profiles for both directions of the current. The yellow (purple, green) area is AFI (FM, NM). Red (blue) solid line in (b) denotes electrons tunnel from left (right) to right (left). The current density used in (b) is $j_e = 2 \times 10^6 \, \mathrm{A \, cm^{-2}}$ and the voltage is $V = 0.2 \, \mathrm{V}$. Other material parameters are [39,40]: $d_{\mathrm{FM1}} = 2d_{\mathrm{FM2}} = 3d_{\mathrm{AFI}} = 3 \, \mathrm{nm}$, $d_{\mathrm{N}} = 30 \, \mathrm{nm}$, $\kappa^{\mathrm{N}} = 401 \, \mathrm{W m^{-1} K^{-1}}$, $\kappa^{\mathrm{F}} = 91 \, \mathrm{W m^{-1} K^{-1}}$, $\kappa^{\mathrm{AF}} = 20 \, \mathrm{W m^{-1} K^{-1}}$, $\sigma^{\mathrm{F}} = 1.43 \times 10^7 \, \mathrm{S m^{-1}}$, $\sigma^{\mathrm{N}} = 5.96 \times 10^7 \, \mathrm{S m^{-1}}$, $\lambda_{\mathrm{inel}} = 1 \, \mathrm{nm}$, and $\alpha = 0.9$ with the choice of Ni as FM, NiO as AFI, and Cu as NM. The temperatures at the outer boundaries of MTJ are kept at 300 K.

also short lived and thus, the annihilation of holes takes place near the interface as well.

Therefore, we may parametrize the heat generation by tunnel electrons as [21,22]

$$P_{\mathrm{re}}(t,x) = \alpha \frac{j_e(t)V(t)}{\lambda_{\mathrm{inel}}} \exp(-|x|/\lambda_{\mathrm{inel}}), \tag{2a}$$

$$P_{\mathrm{em}}(t,x) = (1-\alpha) \frac{j_e(t)V(t)}{\lambda_{\mathrm{inel}}} \exp(-|x|/\lambda_{\mathrm{inel}}), \tag{2b}$$

where $|x|$ is the stack position from AFI/FM interface, α is to parametrize the relative heat power generated in two electrodes, and λ_{inel} is the inelastic scattering mean free path. The parameter α is always larger than 0.5, i.e., the electron-receiving electrode generates more heat; this is because the tunnel probability is larger for tunnel electrons with higher energy.

Since the characteristic time of magnetization dynamics (about picoseconds) is much longer than the electron-electron and electron-phonon collision times (about tens of femtoseconds) which control the rate of change of the temperature [37], we shall solve the above heat diffusion in the steady state

condition, i.e., we assume that the source and temperature become constant once an electric current is turned on. Equation (1) becomes a simple differential form and we are able to find the general solutions for each layer. The integration constants are then determined by boundary conditions in which we use the continuity of the temperature and heat current across the interfaces. In Fig. 2(b) we show the typical temperature profile of tunnel junction by using the materials parameters in bulk form, as indicated in the caption. Since we assume an asymmetric heating parameter $\alpha = 0.9$, i.e., 90% of the Joule heating is generated at the electron receiving electrode, the temperature is always higher for the high voltage side of the junction. The temperature difference across tunnel barrier could reach tens of milli-Kelvin for current density of $j_e = 2 \times 10^6$ A cm^{-2} and voltage of 0.2 V. The actual temperature gradient across the barrier can be even larger when the stack structure and the passivation materials used in the MTJ device are optimized [38].

III. MAGNON CURRENT AND MAGNON TRANSFER TORQUES

With our calculated temperature profile, we now turn to the calculation of magnon current and its induced torque on the free layer. We have previously calculated the giant magneto-spin-Seebeck effect and the magnon transfer torque in all-insulating spin valves in the presence of temperature gradient [41]. It is rather straightforward to extend our calculation for the magnon current in structure made of an antiferromagnetic insulator and magnetic metals.

The magnon current in the presence of a temperature gradient in FM may be written as

$$\mathbf{j}_m^F(x) = -\hbar S_m \nabla_x T(x) \hat{\mathbf{M}}_F - \sigma_m^F \nabla_x \mu_m(x) \hat{\mathbf{M}}_F, \quad (3)$$

where S_m is the spin Seebeck coefficient [26,41], σ_m^F is the magnon conductivity [26,41], we use the effective magnon chemical potential $\boldsymbol{\mu}_m(x)$ to describe the nonequilibrium magnon accumulation [26,41–44], and $\hat{\mathbf{M}}_F$ is the FM magnetization. Within the AFI layer with two sublattices, the magnon Ohm's law is

$$\mathbf{j}_m^{AF}(x) = -\sigma_m^{AF} \nabla_x \boldsymbol{\mu}_m(x), \quad (4)$$

where σ_m^{AF} is the AFI magnon conductivity. It is noted that since we consider easy-axis collinear AFI, two degenerate magnon branches cancels out therefore we do not consider magnon spin Seebeck effect in AFI [28,45].

The exchange interaction at AFI/FM interface is responsible for the magnon transmission

$$H_{int} = -J_{int} \sum_i \mathbf{S}_{i,F} \cdot \mathbf{S}_{i,a(b)}, \quad (5)$$

where J_{int} is the interface exchange constant, $\mathbf{S}_{i,F}$ represents the spin at the interface of FM layer, and $\mathbf{S}_{i,a(b)}$ is the spin of two sublattices of AFI. We here consider that (1) both FM and AFI have in-plane uniaxial anisotropy, and (2) the AFI interface is a compensated one such that the exchange coupling between the ferromagnetic spin and either sublattice spin of the AFI is modeled by the same J_{int}. The order parameter of AFI is assumed to have an angle to the magnetization of FM,

thus the second quantization of Eq. (5) would be

$$H_{int} = -J_{int} \sum_{\mathbf{kq}} (S_F S_{AF})^{1/2} [C_{\mathbf{q}} A_{\mathbf{k}} \alpha_{\mathbf{q}}^\dagger (1 + \hat{\mathbf{n}} \cdot \hat{\mathbf{M}}_F)$$
$$+ C_{\mathbf{q}} A_{\mathbf{k}} \beta_{\mathbf{q}}^\dagger (1 - \hat{\mathbf{n}} \cdot \hat{\mathbf{M}}_F) + \text{H.c.}] \delta_{\mathbf{k},\mathbf{q}}, \quad (6)$$

where $\hat{\mathbf{n}}$ is the AFI order parameter, $A_{\mathbf{k}}$ ($A_{\mathbf{k}}^\dagger$) represents the annihilation (creation) operators for the FM magnons, $\alpha_{\mathbf{q}}^\dagger$, $\alpha_{\mathbf{q}}$ and $\beta_{\mathbf{q}}^\dagger$, $\beta_{\mathbf{q}}$ are the creation and annihilation operators for the two magnon branches of AFI, $C_{\mathbf{q}} = u_{\mathbf{q}} - v_{\mathbf{q}}$ where $u_{\mathbf{q}}$ and $v_{\mathbf{q}}$ are the Bogoliubov transformation coefficients of AFI magnons, $S_{F(AF)}$ is the magnitude of FM (AFI) spin, and we have neglected the high order magnon interactions.

Two sets of boundary conditions at interfaces are needed to determine the integration constants from Eqs. (3) and (4). The first one is that the longitudinal magnon spin current is continuous across the FM/AFI interface,

$$j_m^F = \hat{\mathbf{M}}_F \cdot \mathbf{j}_m^{AF}, \quad (7)$$

and their magnitude is related to the difference of magnon chemical potential at two sides of the interface:

$$j_m = G_{A/F}^\parallel [\mu_m^F - \boldsymbol{\mu}_m^{AF} \cdot \hat{\mathbf{M}}_F], \quad (8)$$

where $G_{A/F}^\parallel$ is the longitudinal magnon spin conductance. For the $\hat{\mathbf{n}} \cdot \hat{\mathbf{M}}_F = 1$ case, the interface exchange interaction in the form of $J_{int} A_{\mathbf{k}} \alpha_{\mathbf{q}}^\dagger$ leads to a spin current across the interface. The longitudinal magnon spin conductance has already been calculated in Ref. [46] and for temperature much lower than the Curie and Néel temperatures, it scales with $\frac{J_{int}^2}{(k_B T_C)(k_B T_N)} (\frac{T}{T_C})^{1/2} (\frac{T}{T_N})^2$.

For the case in which the quantization axis of AFI is perpendicular to local magnetization of FM, e.g., $\hat{\mathbf{n}} \cdot \hat{\mathbf{M}}_F = 0$, we have both $\alpha_{\mathbf{q}}$ and $\beta_{\mathbf{q}}$ that can create a FM magnon with the interaction $J_{int} A_{\mathbf{k}}^\dagger (\alpha_{\mathbf{q}} + \beta_{\mathbf{q}})$. Since $\alpha_{\mathbf{q}}$ and $\beta_{\mathbf{q}}$ have opposite spin direction, the nonequal accumulations of these two magnons would create a transverse spin torque on FM. The second boundary condition would be

$$\hat{\mathbf{M}}_F \times [\hat{\mathbf{M}}_F \times \mathbf{j}_m^{AF}] = -G_{A/F}^\perp \hat{\mathbf{M}}_F \times [\hat{\mathbf{M}}_F \times \boldsymbol{\mu}_m^{AF}], \quad (9)$$

where $G_{A/F}^\perp$ is analogous to the mixing conductance and its magnitude is half the longitudinal one. We show the detailed derivation in the Appendix. Note that the magnon current in FM layers is always parallel to the direction of the magnetization, as in the case of the electron spin current.

With these boundary conditions and the temperature profile we have numerically solved in Sec. II, we can determine the magnon accumulation and magnon current in each layer. The magnon torque on the free layer FM2 is simply identified as the transverse component (relative to the magnetization vector of the FM2) of the magnon current at the AFI/FM2 interface.

IV. AMPLIFICATION OF SPIN TORQUES

To quantitatively estimate the enhancement of the spin torque by using AFI barrier, we numerically calculate the magnon current and obtain the magnon spin torque due to the temperature difference generated by the tunnel electrons.

To be more concrete, we choose the critical torque τ_{cr} for the switching of the free layer that is equivalent to the critical
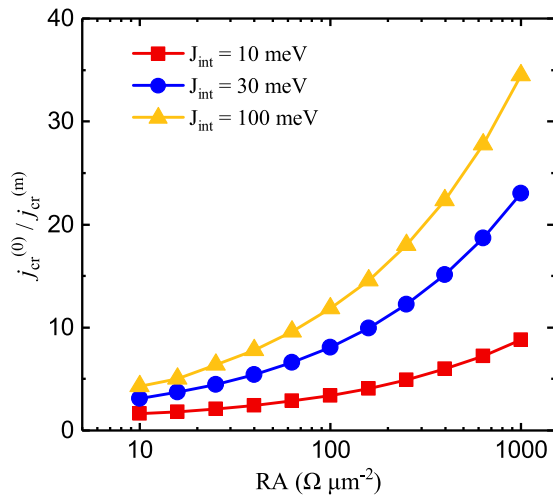
FIG. 3. The dependence of the ratio of the switching current density without and with the magnon spin torques on tunnel resistance area product (RA) at different interface exchange coupling strength. We assume the critical electric current $j_{cr}^{(0)} = 5 \times 10^6$ A cm^{-2} with polarization $P = 0.5$ in the absence of the magnon spin torque. The RA value scales exponentially with the barrier thickness, RA $= 10 \, \Omega \, \mu m^2$ at $d_{AFI} = 1$ nm and RA $= 10^3 \, \Omega \, \mu m^2$ at $d_{AFI} = 2$ nm. Other parameters used in this figure are: $d_{FM1} = 2d_{FM2} = 3$ nm, $T_C = 630$ K, $T_N = 530$ K, $a_F = 0.35$ nm, $a_{AF} = 0.417$ nm, $S_F = S_{AF} = 2$.

electric current $j_{cr}^{(0)} = 5 \times 10^6$ A cm^{-2} in the absence of the magnon spin torque. When the magnon spin torque is turned on, we numerically determine the new critical electric current density $j_{cr}^{(m)}$ needed to generate the *same amount* of torque τ_{cr}. As the magnon torque is directly related to the Joule heating, the relative contribution between magnon current and electron spin current depends highly on the tunnel resistance. The larger the voltage (or the resistance), the greater the magnon torque relative to the electron spin torque.

In Fig. 3 we show the dependence of the ratio of the switching current density without and with the magnon spin torques on tunnel resistance area product (RA) for $\theta = \pi/2$ (the angle between the magnetization directions of the two magnetic layers) at different interface exchange coupling strengths. We note that, in Fig. 3, all lines represent the exact same total torque τ_{cr}: as the resistance and the exchange coupling increase, the magnon spin torque increases, and thus the electric current needed to generate the same total torque reduces.

Clearly a large tunnel resistance generates a larger magnon spin torque and therefore a thicker tunnel barrier is favored. A thick barrier thickness usually improves the tunnel magnetoresistance. However, for device applications, the tunnel resistance has to match with other parts of the electronics and thus we cannot increase the resistance indefinitely.

V. DISCUSSIONS AND CONCLUSIONS

The spin currents, or the angular momentum currents, of tunnel electrons and diffusive magnons, are not always additive. One may simply understand the relative sign of spin and

magnon currents as follows. Consider the magnetization of two magnetic electrodes in parallel. If the majority electrons have a larger tunnel conductance than the minority electrons, the electron spin current would be additive to the magnon current, because the spin direction of magnons is always antiparallel to the majority electrons and the flow direction of magnons from asymmetric tunneling heating is opposite to the (spin) electron current. Thus, it is essential to choose a MTJ in which majority electron tunneling dominates.

We have shown in this paper that there is a theoretical possibility that an AFI-based MTJ could significantly reduce the critical current density compared to nonmagnetic barrier-based MTJ, particularly, the MgO-based MTJ. The major challenge is to identify an AFI barrier that displays a large TMR and other technologically friendly parameters such as tunable tunnel resistance, favorable temperature and bias dependence of TMR, and high transparent AFI for magnons to propagate across. We recall that at the early stage of MTJ development, Ni/NiO/Co junction was reported to have small TMR at low temperature [47]. When the Al$_2$O$_3$-based MTJ with more than 10% room temperature TMR was discovered in 1995, many experimental groups were racing to find better MTJs with a larger TMR value. After the MgO-based MTJs were discovered in 2004, the search for new tunnel junctions was no longer interesting to many groups. Research effort has been focused on optimizing MgO-based MTJs which become the exclusive material choice for all spintronics applications. This work illustrates a need for a completely different MTJ in which the barrier is an antiferromagnetic material. There are many classes of antiferromagnetic insulators and the present work provides a strong motivation for experimental search of AFI-based MTJs.

Our simplified model illustrates the possible advantage of using AFI barrier-based MTJs. However, there are a number of complications. As we have learned that a large TMR of MgO-based MTJ has its origin in the electronic state matching between the MgO layer and the ferromagnetic electrodes for a particular spin channel [5], it is unclear whether a particular AF material would also have this spin-dependent electronic state matching such that an extremely large TMR can be found. We also expect that the orientations of the crystalline and staggered magnetic moments would play an important role for both TMR and the spin/magnon transfer torques. In addition, our study completely ignore the influence of the inelastic scattering in the AFI barrier.

In conclusion, we have demonstrated theoretically that an AFI barrier-based MTJ can achieve a much lower switching current density by "reuse" of the wasted energy of tunnel electrons. The advantage of AFI over NM barrier is that the AFI barrier provides a magnon propagating gateway for additional spin-transfer torques created by the tunnel electrons induced thermal gradient. If a proper AFI-based MTJ is realized experimentally, one would generate a new perspective of lowering switching current density of spin-transfer torque-based MRAMs.

APPENDIX: DERIVATION OF THE INTERFACIAL MAGNON SPIN CONDUCTANCE

Consider the exchange interaction at the interface of antiferromagnet and ferromagnet. The Hamiltonian between two spins would be simply

$$H_{\text{int}} = -J_{\text{int}} \sum_i \mathbf{S}_{i,\text{F}} \cdot \mathbf{S}_{i,a} - J_{\text{int}} \sum_i \mathbf{S}_{i,\text{F}} \cdot \mathbf{S}_{i,b}, \qquad (A1)$$

where $\mathbf{S}_{i,\text{F}}$ represents the ferromagnetic spin and $\mathbf{S}_{i,a(b)}$ is the spin of the two sublattices of collinear antiferromagnet.

We choose plane normal as x axis and the easy axis of FM as along z axis. We assume the easy axis of AFI is in y-z plane but having an angle of to z. Therefore we have the spin rotation as

$$S_{i,a(b)}^x = S_{i,a(b)}^{x'}, \qquad (A2)$$

$$S_{i,a(b)}^y = S_{i,a(b)}^{y'}\hat{\mathbf{n}} \cdot \hat{\mathbf{M}}_{\text{F}} - S_{i,a(b)}^{z'}\hat{\mathbf{n}} \times \hat{\mathbf{M}}_{\text{F}}, \qquad (A3)$$

$$S_{i,a(b)}^z = S_{i,a(b)}^{y'}\hat{\mathbf{n}} \times \hat{\mathbf{M}}_{\text{F}} + S_{i,a(b)}^{z'}\hat{\mathbf{n}} \cdot \hat{\mathbf{M}}_{\text{F}}, \qquad (A4)$$

where $\hat{\mathbf{n}}$ is the Néel order of AFI, $\hat{\mathbf{M}}_{\text{F}}$ is the magnetization of FM, $x'y'z'$ is the local coordinate of AFI, and the easy axis of AF is along z' axis.

We first apply transformation that relate the components of the local spin operators to the creation and annihilation operators of spin deviations,

$$\begin{aligned} H_{\text{int}} = &-\frac{J_{\text{int}}}{4} \sum_i (S_{i,\text{F}}^\dagger S_{i,a(b)}^\dagger + S_{i,\text{F}} S_{i,a(b)})(1 - \hat{\mathbf{n}} \cdot \hat{\mathbf{M}}_{\text{F}}) \\ &+ (S_{i,\text{F}}^\dagger S_{i,a(b)} + S_{i,\text{F}} S_{i,a(b)}^\dagger)(1 + \hat{\mathbf{n}} \cdot \hat{\mathbf{M}}_{\text{F}}) \\ &+ S_{i,\text{F}}^z S_{i,a(b)}^{z'} \hat{\mathbf{n}} \cdot \hat{\mathbf{M}}_{\text{F}} \\ &+ \frac{2}{i}\big[S_{i,\text{F}}^z(S_{i,a(b)}^\dagger - S_{i,a(b)}) - (S_{i,\text{F}}^\dagger - S_{i,\text{F}})S_{i,a(b)}^{z'}\big]\hat{\mathbf{n}} \times \hat{\mathbf{M}}_{\text{F}}. \end{aligned}$$
$$(A5)$$

Within the spin wave approximation, one can express such exchange interaction in terms of boson operators that create or destroy magnons,

$$\begin{aligned} H_{\text{int}} = &\frac{-J_{\text{int}}}{2} \sum_i \sqrt{S_{\text{F}}S_{\text{AF}}}\{[A_i(a_i + b_i^\dagger) + \text{H.c.}](1 - \hat{\mathbf{n}} \cdot \hat{\mathbf{M}}_{\text{F}}) \\ &+ [A_i(a_i^\dagger + b_i) + \text{H.c.}](1 + \hat{\mathbf{n}} \cdot \hat{\mathbf{M}}_{\text{F}})\} \\ &- (S_{\text{F}} - A_i^\dagger A_i)(a_i^\dagger a_i - b_i^\dagger b_i)\hat{\mathbf{n}} \cdot \hat{\mathbf{M}}_{\text{F}} \\ &+ \frac{\sqrt{2}}{i}\{\sqrt{S_{\text{F}}}(A_i - A_i^\dagger)(a_i^\dagger a_i - b_i^\dagger b_i) \\ &+ \sqrt{S_{\text{AF}}}[(S_{\text{F}} - A_i^\dagger A_i)(a_i + b_i^\dagger - \text{H.c.})]\}\hat{\mathbf{n}} \times \hat{\mathbf{M}}_{\text{F}}, \quad (A6) \end{aligned}$$

where we have used the Holstein-Primakoff transformation in linear approximation: $S_{i,\text{F}}^\dagger = \sqrt{2S_{\text{F}}}A_i$, $S_{i,\text{F}}^z = S_{\text{F}} - A_i^\dagger A_i$ for FM and $S_{i,a}^\dagger = \sqrt{2S_{\text{AF}}}a_i$, $S_{z,a}^{z'} = S_{\text{AF}} - a_i^\dagger a_i$, $S_{i,b}^\dagger = \sqrt{2S_{\text{AF}}}b_i^\dagger$, $S_{i,b}^{z'} = -S_{\text{AF}} + b_i^\dagger b_i$. The creation ($A_i^\dagger$, $a_i^\dagger$, and $b_i^\dagger$) and destruction (A_i, a_i, and b_i) operators for spin deviations satisfy the common boson commutation rules.

We proceed by introducing the Fourier transform of the collective boson operators

$$A_i = \frac{1}{\sqrt{N}} \sum_k e^{-i\mathbf{q}\cdot\mathbf{R}_i} A_{\mathbf{q}},$$

$$A_i^\dagger = \frac{1}{\sqrt{N}} \sum_k e^{i\mathbf{q}\cdot\mathbf{R}_i} A_{\mathbf{q}}^\dagger,$$

$$a_i = \frac{1}{\sqrt{N}} \sum_k e^{-i\mathbf{q}\cdot\mathbf{R}_i} a_{\mathbf{q}},$$

$$b_i = \frac{1}{\sqrt{N}} \sum_k e^{-i\mathbf{q}\cdot\mathbf{R}_i} b_{\mathbf{q}},$$

$$a_i^\dagger = \frac{1}{\sqrt{N}} \sum_k e^{i\mathbf{q}\cdot\mathbf{R}_i} a_{\mathbf{q}}^\dagger,$$

$$b_i^\dagger = \frac{1}{\sqrt{N}} \sum_k e^{i\mathbf{q}\cdot\mathbf{R}_i} b_{\mathbf{q}}^\dagger,$$

and the diagonalization of the quadratic part of the AF Hamiltonian

$$a_{\mathbf{q}} = u_{\mathbf{q}}\alpha_{\mathbf{q}} - v_{\mathbf{q}}\beta_{-\mathbf{q}}^\dagger,$$

$$b_{\mathbf{q}}^\dagger = -v_{-\mathbf{q}}\alpha_{-\mathbf{q}} + u_{-\mathbf{q}}\beta_{\mathbf{q}}^\dagger,$$

$$a_{\mathbf{q}}^\dagger = u_{\mathbf{q}}\alpha_{\mathbf{q}}^\dagger - v_{\mathbf{q}}\beta_{-\mathbf{q}},$$

$$b_{\mathbf{q}} = -v_{-\mathbf{q}}\alpha_{-\mathbf{q}}^\dagger + u_{-\mathbf{q}}\beta_{\mathbf{q}},$$

where N is the number of spins and the coefficients satisfies $u_{\mathbf{q}}^2 - v_{\mathbf{q}}^2 = 1$.

Therefore the second quantization of the interfacial Hamiltonian is

$$\begin{aligned} H_{\text{int}} = &-J_{\text{int}} \sum_{\mathbf{kq}} (S_{\text{F}}S_{\text{AF}})^{1/2}[C_{\mathbf{q}}A_{\mathbf{k}}\alpha_{\mathbf{q}}^\dagger(1 + \hat{\mathbf{n}} \cdot \hat{\mathbf{M}}_{\text{F}}) \\ &+ C_{\mathbf{q}}A_{\mathbf{k}}\beta_{\mathbf{q}}^\dagger(1 - \hat{\mathbf{n}} \cdot \hat{\mathbf{M}}_{\text{F}}) + \text{H.c.}]\delta_{\mathbf{k},\mathbf{q}}, \qquad (A7) \end{aligned}$$

where we have neglected the high order magnon interactions.

It would be straightforward to calculate the longitudinal and transverse spin current across AF/F interface (per interface cross area A_{I}) by using the Fermi's golden rule

$$j_{\text{AF/F}} = \left\langle \frac{1}{iA_{\text{I}}}\left[\sum_{\mathbf{q}} a_{\mathbf{q}}^\dagger a_{\mathbf{q}}, H_{\text{int}}\right]\right\rangle, \qquad (A8)$$

where $\langle \rangle$ refers to the thermal averaging over all states. Using the rough interface approximation, we find

$$j_{\text{AF/F}}^{\parallel} = G_{\text{AF/F}}^{\parallel}\big(\mu_m^{\text{F}} - \mu_m^{\alpha}\big), \qquad (A9)$$

$$j_{\text{AF/F}}^{\perp} = G_{\text{AF/F}}^{\perp}\big[\mu_m^{\text{F}} - \big(\mu_m^{\alpha} - \mu_m^{\beta}\big)\big], \qquad (A10)$$

where the magnon conductance is

$$\begin{aligned} G_{\text{AF/F}}^{\parallel} = 2G_{\text{AF/F}}^{\perp} = &\frac{\pi S_{\text{F}}S_{\text{AF}}J_{\text{int}}^2 a_{\text{F}}^2 a_{\text{AF}}^2}{2k_B T} \int d\varepsilon_{\mathbf{q}} d\varepsilon_{\mathbf{q}'} (u_{\mathbf{q}} - v_{\mathbf{q}}) \\ &\times g_m^{\text{F}}(\varepsilon_{\mathbf{q}})g_m^{\text{AF}}(\varepsilon_{\mathbf{q}})\text{csch}^2 \frac{\varepsilon_{\mathbf{q}}}{2k_B T}, \qquad (A11) \end{aligned}$$

where $a_{\text{F(AF)}}$ is the lattice constant of the FM (AFI) material and g_m is the density of states of magnon.

[1] M. Julliere, Tunneling between ferromagnetic films, Phys. Lett. A **54**, 225 (1975).

[2] J. C. Slonczewski, Conductance and exchange coupling of two ferromagnets separated by a tunneling barrier, Phys. Rev. B **39**, 6995 (1989).

[3] J. S. Moodera, L. R. Kinder, T. M. Wong, and R. Meservey, Large Magnetoresistance at Room Temperature in Ferromagnetic Thin Film Tunnel Junctions, Phys. Rev. Lett. **74**, 3273 (1995).

[4] T. Miyazaki and N. Tezuka, Giant magnetic tunneling effect in Fe/Al$_2$O$_3$/Fe junction, J. Magn. Magn. Mater. **139**, L231 (1995).

[5] W. H. Butler, X.-G. Zhang, T. C. Schulthess, and J. M. MacLaren, Spin-dependent tunneling conductance of Fe|MgO|Fe sandwiches, Phys. Rev. B **63**, 054416 (2001).

[6] J. Mathon and A. Umerski, Theory of tunneling magnetoresistance of an epitaxial Fe/MgO/Fe(001) junction, Phys. Rev. B **63**, 220403 (2001).

[7] S. S. P. Parkin, C. Kaiser, A. Panchula, P. M. Rice, B. Hughes, M. Samant, and S.-H. Yang, Giant tunnelling magnetoresistance at room temperature with MgO (100) tunnel barriers, Nat. Mater. **3**, 862 (2004).

[8] S. Yuasa, T. Nagahama, A. Fukushima, Y. Suzuki, and K. Ando, Giant room-temperature magnetoresistance in single-crystal Fe/MgO/Fe magnetic tunnel junctions, Nat. Mater. **3**, 868 (2004).

[9] D. Apalkov, B. Dieny, and J. M. Slaughter, Magnetoresistive random access memory, Proc. IEEE **104**, 1796 (2016).

[10] S. Ikeda, J. Hayakawa, Y. Ashizawa, Y. M. Lee, K. Miura, H. Hasegawa, M. Tsunoda, F. Matsukura, and H. Ohno, Tunnel magnetoresistance of 604% at 300 K by suppression of Ta diffusion in Co Fe B/Mg O/Co Fe B pseudo-spin-valves annealed at high temperature, Appl. Phys. Lett. **93**, 082508 (2008).

[11] B. N. Engel, J. Akerman, B. Butcher, R. W. Dave, M. DeHerrera, M. Durlam, G. Grynkewich, J. Janesky, S. V. Pietambaram, N. D. Rizzo, J. M. Slaughter, K. Smith, J. J. Sun, and S. Tehrani, A 4-Mb toggle MRAM based on a novel bit and switching method, IEEE Trans. Magn. **41**, 132 (2005).

[12] J. C. Slonczewski, Current-driven excitation of magnetic multilayers, J. Magn. Magn. Mater. **159**, L1 (1996).

[13] L. Berger, Emission of spin waves by a magnetic multilayer traversed by a current, Phys. Rev. B **54**, 9353 (1996).

[14] G. D. Fuchs, N. C. Emley, I. N. Krivorotov, P. M. Braganca, E. M. Ryan, S. I. Kiselev, J. C. Sankey, D. C. Ralph, R. A. Buhrman, and J. A. Katine, Spin-transfer effects in nanoscale magnetic tunnel junctions, Appl. Phys. Lett. **85**, 1205 (2004).

[15] Y. Huai, F. Albert, P. Nguyen, M. Pakala, and T. Valet, Observation of spin-transfer switching in deep submicron-sized and low-resistance magnetic tunnel junctions, Appl. Phys. Lett. **84**, 3118 (2004).

[16] M. Hosomi, H. Yamagishi, T. Yamamoto, K. Bessho, Y. Higo, K. Yamane, H. Yamada, M. Shoji, H. Hachino, C. Fukumoto, H. Nagao, and H. Kano, A novel nonvolatile memory with Spin torque transfer magnetization switching: Spin-RAM, in *IEEE International Electron Devices Meeting, 2005, IEDM Technical Digest, Washington, DC* (IEEE, Piscataway, NJ, 2005), pp. 459–462.

[17] S. Ikeda, K. Miura, H. Yamamoto, K. Mizunuma, H. D. Gan, M. Endo, S. Kanai, J. Hayakawa, F. Matsukura, and H. Ohno, A perpendicular-anisotropy CoFeB–MgO magnetic tunnel junction, Nat. Mater. **9**, 721 (2010).

[18] D. C. Worledge, G. Hu, D. W. Abraham, J. Z. Sun, P. L. Trouilloud, J. Nowak, S. Brown, M. C. Gaidis, E. J. O'Sullivan, and R. P. Robertazzi, Spin torque switching of perpendicular Ta | CoFeB | MgO-based magnetic tunnel junctions, Appl. Phys. Lett. **98**, 022501 (2011).

[19] J. Hong and D. L. Mills, Theory of the spin dependence of the inelastic mean free path of electrons in ferromagnetic metals: A model study, Phys. Rev. B **59**, 13840 (1999).

[20] J. Hong and D. L. Mills, Spin dependence of the inelastic electron mean free path in Fe and Ni: Explicit calculations and implications, Phys. Rev. B **62**, 5589 (2000).

[21] R. C. Sousa, I. L. Prejbeanu, D. Stanescu, B. Rodmacq, O. Redon, B. Dieny, J. Wang, and P. P. Freitas, Tunneling hot spots and heating in magnetic tunnel junctions, J. Appl. Phys. **95**, 6783 (2004).

[22] E. Gapihan, J. Hérault, R. C. Sousa, Y. Dahmane, B. Dieny, L. Vila, I. L. Prejbeanu, C. Ducruet, C. Portemont, K. Mackay, and J. P. Nozières, Heating asymmetry induced by tunneling current flow in magnetic tunnel junctions, Appl. Phys. Lett. **100**, 202410 (2012).

[23] J. Xiao, G. E. W. Bauer, K.-c. Uchida, E. Saitoh, and S. Maekawa, Theory of magnon-driven spin Seebeck effect, Phys. Rev. B **81**, 214418 (2010).

[24] H. Adachi, J.-i. Ohe, S. Takahashi, and S. Maekawa, Linear-response theory of spin Seebeck effect in ferromagnetic insulators, Phys. Rev. B **83**, 094410 (2011).

[25] H. Adachi, K.-i. Uchida, E. Saitoh, and S. Maekawa, Theory of the spin Seebeck effect, Rep. Prog. Phys. **76**, 036501 (2013).

[26] S. M. Rezende, R. L. Rodríguez-Suárez, R. O. Cunha, A. R. Rodrigues, F. L. A. Machado, G. A. Fonseca Guerra, J. C. Lopez Ortiz, and A. Azevedo, Magnon spin-current theory for the longitudinal spin-Seebeck effect, Phys. Rev. B **89**, 014416 (2014).

[27] M. Beens, J. P. Heremans, Y. Tserkovnyak, and R. A. Duine, Magnons versus electrons in thermal spin transport through metallic interfaces, J. Phys. D: Appl. Phys. **51**, 394002 (2018).

[28] Y. Ohnuma, H. Adachi, E. Saitoh, and S. Maekawa, Spin Seebeck effect in antiferromagnets and compensated ferrimagnets, Phys. Rev. B **87**, 014423 (2013).

[29] H. Wang, C. Du, P. C. Hammel, and F. Yang, Antiferromagnonic Spin Transport from Y$_3$Fe$_5$O$_{12}$ into NiO, Phys. Rev. Lett. **113**, 097202 (2014).

[30] C. Hahn, G. de Loubens, V. V. Naletov, J. B. Youssef, O. Klein, and M. Viret, Conduction of spin currents through insulating antiferromagnetic oxides, Europhys. Lett. **108**, 57005 (2014).

[31] S. M. Rezende, R. L. Rodríguez-Suárez, and A. Azevedo, Theory of the spin Seebeck effect in antiferromagnets, Phys. Rev. B **93**, 014425 (2016).

[32] S. M. Rezende, R. L. Rodríguez-Suárez, and A. Azevedo, Diffusive magnonic spin transport in antiferromagnetic insulators, Phys. Rev. B **93**, 054412 (2016).

[33] W. Lin, K. Chen, S. Zhang, and C. L. Chien, Enhancement of Thermally Injected Spin Current through an Antiferromagnetic Insulator, Phys. Rev. Lett. **116**, 186601 (2016).

[34] Z. Qiu, J. Li, D. Hou, E. Arenholz, A. T. N'Diaye, A. Tan, K.-i. Uchida, K. Sato, S. Okamoto, Y. Tserkovnyak, Z. Q. Qiu, and E. Saitoh, Spin-current probe for phase transition in an insulator, Nat. Commun. **7**, 12670 (2016).

[35] Y.-M. Hung, C. Hahn, H. Chang, M. Wu, H. Ohldag, and A. D. Kent, Spin transport in antiferromagnetic NiO and magnetoresistance in $Y_3Fe_5O_{12}$/NiO/Pt structures, AIP Adv. **7**, 055903 (2016).

[36] V. Baltz, A. Manchon, M. Tsoi, T. Moriyama, T. Ono, and Y. Tserkovnyak, Antiferromagnetic spintronics, Rev. Mod. Phys. **90**, 015005 (2018).

[37] E. Beaurepaire, J.-C. Merle, A. Daunois, and J.-Y. Bigot, Ultrafast Spin Dynamics in Ferromagnetic Nickel, Phys. Rev. Lett. **76**, 4250 (1996).

[38] A. Deschenes, S. Muneer, M. Akbulut, A. Gokirmak, and H. Silva, Analysis of self-heating of thermally assisted spin-transfer torque magnetic random access memory, Beilstein J. Nanotechnol. **7**, 1676 (2016).

[39] R. W. Powell, R. P. Tye, and M. J. Hickman, The thermal conductivity of nickel, Int. J. Heat Mass Transf. **8**, 679 (1965).

[40] J. E. Keem and J. M. Honig, Selected electrical and thermal properties of undoped nickel oxide, CINDAS Report 52, West Lafayette, Indiana, Aug 1978, https://apps.dtic.mil/dtic/tr/fulltext/u2/a128940.pdf.

[41] Y. Cheng, K. Chen, and S. Zhang, Giant magneto-spin-Seebeck effect and magnon transfer torques in insulating spin valves, Appl. Phys. Lett. **112**, 052405 (2018).

[42] S. S.-L. Zhang and S. Zhang, Magnon Mediated Electric Current Drag Across a Ferromagnetic Insulator Layer, Phys. Rev. Lett. **109**, 096603 (2012).

[43] S. A. Bender, R. A. Duine, and Y. Tserkovnyak, Electronic Pumping of Quasiequilibrium Bose-Einstein-Condensed Magnons, Phys. Rev. Lett. **108**, 246601 (2012).

[44] Y. Cheng, K. Chen, and S. Zhang, Interplay of magnon and electron currents in magnetic heterostructure, Phys. Rev. B **96**, 024449 (2017).

[45] S. M. Wu, W. Zhang, A. KC, P. Borisov, J. E. Pearson, J. S. Jiang, D. Lederman, A. Hoffmann, and A. Bhattacharya, Antiferromagnetic Spin Seebeck Effect, Phys. Rev. Lett. **116**, 097204 (2016).

[46] K. Chen, W. Lin, C. L. Chien, and S. Zhang, Temperature dependence of angular momentum transport across interfaces, Phys. Rev. B **94**, 054413 (2016).

[47] S. Maekawa and U. Gafvert, Electron tunneling between ferromagnetic films, IEEE Trans. Magn. **18**, 707 (1982).